A Theoretical Investigation of the Effects of Sinusoidal Topography on Particle Deposition

J. E. STOUT, Y.-L. LIN, AND S. P. S. ARYA

Department of Marine, Earth, and Atmospheric Sciences, North Carolina State University, Raleigh, North Carolina

(Manuscript received 8 July 1992, in final form 8 February 1993)

ABSTRACT

Trajectories of 500- and 1000-μm diameter particles are calculated as they fall through the spatially varying flow field above sinusoidal terrain for various combinations of atmospheric stability, wind speed, and terrain wavelength. In each case, a set of 20 uniformly spaced particles are released simultaneously above sinusoidal topography and their trajectories are obtained numerically by coupling a linear wave solution for flow over sinusoidal topography with equations for particle motion. The flow field and the associated patterns of deposition are shown to be strongly influenced by atmospheric stratification. For strong stratification, the presence of vertically propagating waves produces relatively concentrated "particle streams." For less stratified conditions with evanescent waves, little focusing of particle trajectories is apparent. The ability of the atmosphere to focus or concentrate falling particles may ultimately produce regions along the surface with enhanced deposition.

1. Introduction

Prediction of particle deposition in the atmosphere is important in many diverse fields of science. Meteorological studies of precipitation patterns primarily involve the fall of raindrops or ice particles (Hobbs et al. 1973). Air pollution studies often involve the deposition of particulate matter generated by industry (Pasquill 1974). Geologists often study the deposition of ash and cinders downwind of volcanic eruptions (Cotton 1944). Soil scientists study the formation of soils from the settling of aeolian grains of sand and dust (Greeley and Iversen 1985). Areas of study such as these could benefit from an improved understanding of particle deposition across complex terrain.

As particles fall toward the surface of the earth, they move under the combined influence of gravitational and aerodynamic forces. For uniform flow over flat land, particles generally fall toward the surface at a constant angle defined by the wind speed and terminal fall velocity of the particle. Above complex terrain, particles fall through a more complex and spatially varying flow field, characterized by terrain-induced velocity perturbations. Particles falling through such a flow field experience a constantly changing fluid dynamic force that may substantially alter their path. Particles that fall from different initial positions will take different paths through the flow field, and thereby experience a different time history of fluid dynamic forces. Under the right conditions, a set of particles may be significantly redistributed relative to one another, producing alternating regions of enhanced and reduced concentration.

The objective of this work is to explore the conditions that bring about a substantial modification of otherwise uniform deposition by calculating the path of particles falling through the flow field above a sinusoidal surface. As discussed in section 2, this is accomplished by coupling a linear wave solution for flow over sinusoidal topography with equations for particle motion. A simple explicit scheme is then applied to calculate the particle trajectories. In section 3, the results from the simulations are presented and the effects of stratification, particle size, wind speed, and terrain wavelength are discussed. Concluding remarks are made in section 4.

2. Theory

A simple method of predicting particle movement is to assume that each particle moves horizontally as the wind, and falls vertically at its terminal velocity relative to the wind (Hobbs et al. 1973). In the limiting case of small light particles within a slowly varying flow field this assumption may be sufficiently accurate. For the opposite extreme of large heavy particles within a rapidly varying flow field the assumption fails. Thus, such a model is not generally applicable to all particle and flow field combinations.

A more rigorous method of particle trajectory prediction is to simply calculate the motion of each particle based upon its natural reaction to applied fluid dynamic and gravitational forces. In this case the particle motion is not artificially constrained; rather, it is predicted from physically based equations of particle motion.

Such a model must contain two essential components: a means of predicting fluid motion at any point

Corresponding author address: Dr. S. P. Arya, Dept. of Marine, Earth and Atmospheric Science, North Carolina State University, P.O. Box 8208, Raleigh, NC 27695-8208.

above the terrain, and a means of predicting particle motion due to the forces that result from the relative movement of the particle through the spatially varying flow field.

a. Flow field over sinusoidal topography

Notation for two-dimensional flow over sinusoidal terrain is defined in Fig. 1. The surface is described by a simple sinusoidal function with terrain amplitude, h_m, and terrain wavelength, L:

$$h(x) = h_m \sin(kx). \tag{1}$$

The horizontal component of wind velocity, u, is aligned with coordinate x and may be expressed as the sum of a basic wind speed, U, plus a terrain-induced perturbation, $u'(x, z)$. The vertical component, w, is aligned with coordinate z and is composed solely of a terrain-induced perturbation, $w'(x, z)$.

The wind velocity field above sinusoidal terrain was derived from linear theory by Queney (1947) and later summarized by Smith (1979). The derived analytical solutions require small amplitude sinusoidal terrain with steady, inviscid, Boussinesq, and nonrotating flow. In addition, the atmosphere is assumed stable with constant stratification. The response of the flow depends upon the relative magnitude of the terrain wavenumber, $k = 2\pi/L$, compared to the Scorer parameter, $l = N/U$, where N is the Brunt–Väisälä frequency.

For the case of strong wind in a weakly stratified atmosphere and a narrow hill, ($l^2 < k^2$), the wind field above sinusoidal terrain may be written as

$$u(x, z) = U(1 + \sqrt{k^2 - l^2}h_m \sin(kx)e^{-\sqrt{k^2 - l^2}z}) \tag{2}$$

$$w(x, z) = kUh_m \cos(kx)e^{-\sqrt{k^2 - l^2}z}. \tag{3}$$

In this case, the terrain-induced disturbance decays exponentially with height, as shown in the upper frame of Fig. 2, and thus, significant flow perturbations are limited to a narrow region close to the surface. The resulting wave field is appropriately classified as evanescent.

For weak wind in strong stratification over a series of wide hills, ($l^2 > k^2$), the wind field above sinusoidal terrain may be written as

$$u(x, z) = U[1 - \sqrt{l^2 - k^2}h_m \cos(kx + \sqrt{l^2 - k^2}z)] \tag{4}$$

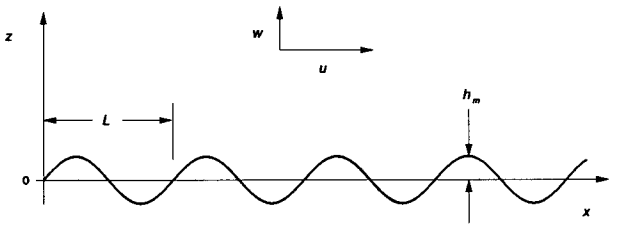

FIG. 1. Definition sketch for flow over sinusoidal topography.

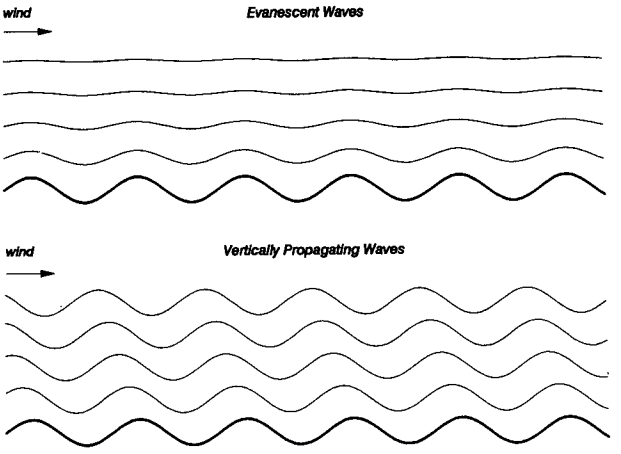

FIG. 2. Examples of evanescent and vertically propagating waves above sinusoidal terrain.

$$w(x, z) = kUh_m \cos(kx + \sqrt{l^2 - k^2}z). \tag{5}$$

In this case, the terrain-induced disturbance propagates upward. The wind field consists of a series of vertically propagating waves with a characteristic upwind phase tilt, as shown in the lower frame of Fig. 2. In this case, the wave amplitude and terrain-induced flow perturbations do not diminish with height.

b. Dynamics of falling particles

The gravitational force acting on a particle of diameter D and density ρ_p falling through air of density ρ may be expressed as

$$F_g = \frac{\pi D^3}{6} g(\rho - \rho_p). \tag{6}$$

The primary fluid dynamic force acting on a nonspinning spherical particle is the aerodynamic drag force, which results from the relative movement of air past the particle. The drag of spherical particles have been studied extensively in the past. At any instant, the resultant drag force acts in the direction of the total relative wind vector. For a particle with frontal area A and drag coefficient C_D, the horizontal and vertical components of the aerodynamic force may be expressed as

$$F_x = C_D A \frac{1}{2} \rho V_{\text{rel}} \left(u - \frac{dX}{dt}\right) \tag{7}$$

$$F_z = C_D A \frac{1}{2} \rho V_{\text{rel}} \left(w - \frac{dZ}{dt}\right). \tag{8}$$

The relative wind speed is defined as

$$V_{\text{rel}} = \left[\left(u - \frac{dX}{dt}\right)^2 + \left(w - \frac{dZ}{dt}\right)^2\right]^{1/2}, \tag{9}$$

where the horizontal and vertical position of the particle is denoted by uppercase X and Z, respectively.

TABLE 1. Drag coefficient of a sphere as a function of Reynolds number, from Morsi and Alexander (1972).

Drag coefficient	Reynolds number range
$C_D = 24.0/\mathrm{Re}$	$\mathrm{Re} < 0.1$
$C_D = 22.73/\mathrm{Re} + 0.0903/\mathrm{Re}^2 + 3.69$	$0.1 < \mathrm{Re} < 1$
$C_D = 29.1667/\mathrm{Re} - 3.8889/\mathrm{Re}^2 + 1.222$	$1 < \mathrm{Re} < 10$
$C_D = 46.5/\mathrm{Re} - 116.67/\mathrm{Re}^2 + 0.6167$	$10 < \mathrm{Re} < 100$
$C_D = 98.33/\mathrm{Re} - 2778.0/\mathrm{Re}^2 + 0.3644$	$100 < \mathrm{Re} < 1000$
$C_D = 148.62/\mathrm{Re} - 47500.0/\mathrm{Re}^2 + 0.357$	$1000 < \mathrm{Re} < 5000$
$C_D = -490.546/\mathrm{Re} + 578700/\mathrm{Re}^2 + 0.46$	$5000 < \mathrm{Re} < 10\,000$
$C_D = -1662.5/\mathrm{Re} + 5416700/\mathrm{Re}^2 + 0.519$	$10\,000 < \mathrm{Re} < 50\,000$

If a particle is moving at the same speed as the wind, then the aerodynamic force vanishes. This suggests that if the wind speed or direction changes suddenly, the particle must translate relative to the wind before a force can be generated to change the velocity of the particle. The amount of relative movement between the particle and air depends upon the size and mass of the particle as well as the magnitude and frequency of the wind fluctuations. In the limiting case of small lightweight particles in a slowly varying flow field there is little relative movement required to produce forces sufficient to move the tiny particle, and so the particle tends to follow the motion of the fluid quite closely. At the opposite extreme of large heavy particles falling through a rapidly varying flow field a particle rarely follows the exact motion of the fluid.

The drag coefficient of a sphere, C_D, varies appreciably with Reynolds number, Re, where

$$\mathrm{Re} = \frac{\rho V_{\mathrm{rel}} D}{\mu}. \tag{10}$$

Morsi and Alexander (1972) developed a set of regression equations (shown in Table 1) that allow the calculation of drag coefficient for a sphere for a large range of Reynolds number. This set of equations results from an empirical fit to the standard drag curve for spheres shown in Fig. 3.

At this point we link the equations that govern particle motion with the equations that describe the wind field. Gravity and drag forces acting on a particle have been defined by Eqs. (6), (7), and (8). The velocity field above the terrain is defined by either Eqs. (2) and (3) or Eqs. (4) and (5), depending mainly upon atmospheric stability. Summing all the wind drag and gravitational forces and dividing by particle mass yields the following expressions for the horizontal and vertical components of particle acceleration,

$$\frac{d^2X}{dt^2} = \frac{3}{4}\frac{\rho}{\rho_p}\frac{C_D}{D} V_{\mathrm{rel}}\left(u - \frac{dX}{dt}\right) \tag{11}$$

$$\frac{d^2Z}{dt^2} = g\frac{(\rho - \rho_p)}{\rho_p} + \frac{3}{4}\frac{\rho}{\rho_p}\frac{C_D}{D} V_{\mathrm{rel}}\left(w - \frac{dZ}{dt}\right). \tag{12}$$

The motion of each particle is calculated by using a simple explicit numerical scheme that is iterated over numerous small time steps ($\Delta t = 0.05$ s). The position of the particle as a function of time is calculated as follows:

$$X^{\tau+1} = X^{\tau} + \left(\frac{dX}{dt}\right)^{\tau}\Delta t + \frac{1}{2}\left(\frac{d^2X}{dt^2}\right)^{\tau}\Delta t^2 \tag{13}$$

$$Z^{\tau+1} = Z^{\tau} + \left(\frac{dZ}{dt}\right)^{\tau}\Delta t + \frac{1}{2}\left(\frac{d^2Z}{dt^2}\right)^{\tau}\Delta t^2 \tag{14}$$

and the velocity of the particle as a function of time is calculated as follows:

$$\left(\frac{dX}{dt}\right)^{\tau+1} = \left(\frac{dX}{dt}\right)^{\tau} + \left(\frac{d^2X}{dt^2}\right)^{\tau}\Delta t \tag{15}$$

$$\left(\frac{dZ}{dt}\right)^{\tau+1} = \left(\frac{dZ}{dt}\right)^{\tau} + \left(\frac{d^2Z}{dt^2}\right)^{\tau}\Delta t, \tag{16}$$

where the superscript τ denotes the time step.

Particles are released with no initial vertical velocity and with horizontal velocity equal to that of the basic wind, U. The new position and velocity of the particle at time step $\tau + 1$ are computed from Eqs. (13) through (16) from values of particle velocity and particle acceleration at time step τ. The particle velocity components, dX/dt and dZ/dt, are known at each time step either from the given initial conditions or from the calculation of Eqs. (15) and (16) at the previous time step. The particle acceleration components, d^2X/dt^2 and d^2Z/dt^2, are calculated from Eqs. (11) and (12) from known values of particle speed and wind velocity at time step τ. The wind velocity components, u and w, are calculated at the current position of the particle at time step τ from Eqs. (2) and (3) or (4) and (5), depending mainly upon atmospheric stability. This process is repeated until the height of the particle is equal to the height of the local terrain.

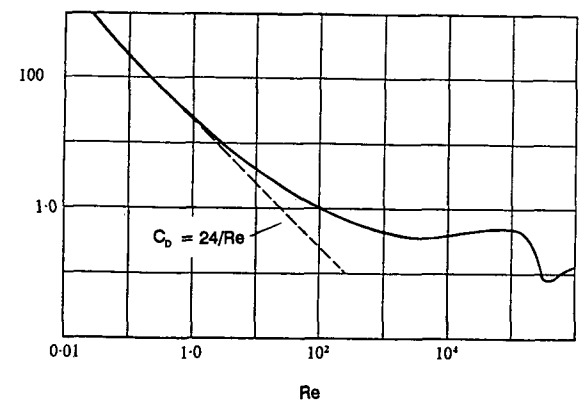

FIG. 3. Drag coefficient of a sphere as a function of Reynolds number. (After Morsi and Alexander 1972.)

TABLE 2. Comparison of terminal velocity calculated with the present model and measured by Gunn and Kinzer (1949) for $\rho = 1.19$ kg m^{-3} and $\nu = 1.53 \times 10^{-5}$ m^2 s^{-1}.

Diameter (mm)	Terminal velocity (m s^{-1})	
	Calculated	Measured
0.25	0.94	—
0.30	1.18	1.17
0.40	1.65	1.62
0.50	2.09	2.06
0.60	2.48	2.47
0.70	2.85	2.87
0.80	3.23	3.27
0.90	3.61	3.67
1.00	3.98	4.03

3. Results

One simple test of the model is to set the wind speed to zero and let particles of different size fall vertically until the drag force just balances the gravitational force. Under this condition a particle falls at its terminal velocity, w_t.

Gunn and Kinzer (1949) have experimentally measured the terminal velocity of water drops. Table 2 shows a comparison of the numerical model and this experimental data. The satisfactory agreement suggests that the model works sufficiently well for particles falling through a quiescent atmosphere.

Another test of the model is to check the angle of fall for particles falling toward a flat surface within a uniform wind current. Regardless of the initial velocity of the particle, under such uniform and steady flow conditions particles eventually fall at their terminal velocity, w_t, while they drift horizontally at the speed of the wind, U. Each particle falls at a constant angle, α, where α may be expressed as

$$\alpha = \tan^{-1}\left(\frac{|w_t|}{U}\right). \tag{17}$$

The numerical model makes no assumptions about the horizontal drift velocity matching that of the wind, nor does it assume that the particles fall at their terminal velocity. Rather, it simply calculates the resulting motion of the particles based upon the applied forces. In this uniform and steady flow case, however, the fall angle predicted by the numerical model should match the value computed from Eq. (17), thus providing a test of the numerical model's validity. The numerically computed trajectories are shown in Fig. 4 for particle diameters of 0.5 and 1.0 mm falling toward flat terrain. The particles are released with initial horizontal velocity equal to U (10 m s^{-1}) and no vertical velocity. It is clear from this figure that the particles quickly achieve terminal velocity and fall at the correct angle predicted by Eq. (17), namely, 11.8° for particle diameter of 0.5 mm and 21.7° for particle diameter of 1.0 mm. Thus, the numerical model correctly predicts the angle of fall over flat terrain.

Next we consider sinusoidal terrain. In each case, 20 particles, distributed uniformly across two terrain wavelengths, are released simultaneously from a height

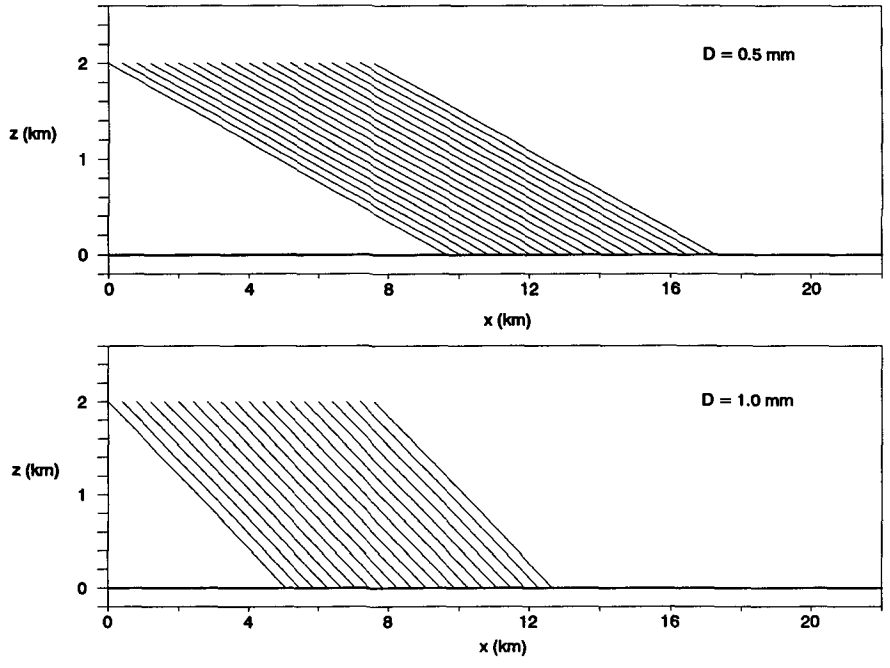

FIG. 4. Particle trajectories over flat land.

TABLE 3. Test summary for flow over sinusoidal terrain for evanescent (EVN) and vertically propagating (VP) waves.

Case	Wave type	L (km)	h_m (m)	U (m s^{-1})	N (s^{-1})	l (m^{-1})	k (m^{-1})	Maximum u'/U	Maximum w'/U	D (mm)
C1	EVN	4	200	10	0.01	0.001	0.0016	0.24	0.31	1.0
C2	VP	4	200	10	0.02	0.002	0.0016	0.24	0.31	1.0
C3	EVN	4	200	10	0.01	0.001	0.0016	0.24	0.31	0.5
C4	VP	4	200	10	0.02	0.002	0.0016	0.24	0.31	0.5
C5	VP	4	200	5	0.01	0.002	0.0016	0.24	0.31	1.0
C6	VP	8	200	10	0.01	0.001	0.0008	0.12	0.16	1.0

of 2000 m. In all cases particle density, ρ_p, is 1000 kg m^{-3}, which corresponds to the density of water. Particles are released with a horizontal velocity equal to the basic wind speed, U, but are given no initial vertical velocity.

Table 3 gives a summary of the six test cases. Case C1 is considered the base case. Most of the other cases are a single perturbation of only one variable from the base case.

a. *Effect of stratification*

Cases C1 and C2, shown in Fig. 5, are identical except that $N = 0.01$ s^{-1} in case C1, whereas $N = 0.02$ s^{-1} in case C2. By doubling the Brunt–Väisälä frequency, the mode of wave propagation is changed from evanescent waves in C1 to vertically propagating waves in C2. This distinct change in wave regime has a noticeable effect on the resulting particle trajectories. In case C2 a concentrated particle stream is evident, which results from the bunching or focusing of particle path lines. On the other hand, in case C1 a concentrated particle stream is not discernible.

This striking difference in particle behavior is a direct consequence of the fundamental differences in the flow field, as revealed by the streamlines. For evanescent waves, shown in case C1, the amplitude decreases exponentially with height such that only near the surface are the streamlines significantly perturbed. For vertically propagating waves, shown in case C2, the amplitude does not decrease with height so that significant particle accelerations occur along the entire trajectory, not just near the surface.

Another significant difference in the flow fields is the orientation of the constant phase lines. For evanescent waves (C1) the constant phase lines are vertical whereas for vertically propagating waves (C2) the constant phase lines tilt upwind. Thus, for vertically propagating waves the constant phase lines are more closely aligned with the natural fall angle of the particles.

For vertically propagating waves, constant phase lines that pass through either wave peaks or troughs

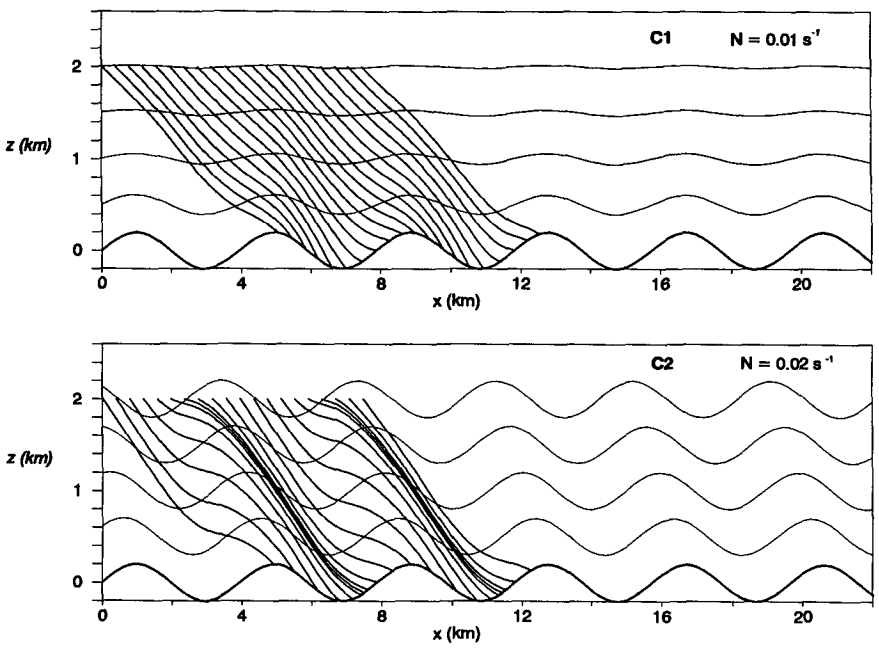

FIG. 5. Effect of stratification on particle trajectories over sinusoidal terrain.

correspond to the dividing line between regions of positive and negative vertical velocity. Particles fall more slowly in regions of positive w and so the trajectories appear more horizontal. The mean flow sweeps these particles into regions of negative w where the trajectories are steeper. If the constant phase lines are closely aligned with the natural fall line of the particles then particles tend to remain in regions of positive w for longer periods of time. If the lines of constant phase are not well aligned with the natural fall angle of the particles then particles pass rapidly through regions of positive and negative w, allowing less time for redistribution to occur. One may conclude that holding all other factors constant, the closer the natural fall line coincides with the lines of constant phase, the more pronounced will be the convergence of particle path lines.

b. *Effect of particle size*

Figures 6 and 7 show the effect of reducing the diameter of each particle from 1 mm to 0.5 mm for evanescent and vertically propagating waves, respectively. Reducing the particle size reduces the fall velocity of the particles; thus, they move farther downrange as the particle size is reduced. As a result, each individual trajectory stretches across an additional terrain wavelength, which induces more waviness in each path line.

A smaller particle is generally more responsive to wind fluctuations. Therefore, if a flow field tends to produce concentrated particle streams, smaller particles should be focused more quickly than larger particles. For evanescent waves, shown in Fig. 6, there are no significant particle streams for either particle size. One may conclude that, regardless of the particle size, evanescent wave fields are not effective at producing concentrated particle streams. On the other hand, for small particles in vertically propagating waves, shown in Fig. 7, there appear to be regions of rapid formation of particle streams alternating with regions where trajectories diverge slightly. This indicates that the smaller particles are responding rapidly to the local wind field and the wind field is effective at producing particle streams.

c. *Effect of wind speed*

Figure 8 shows the effect of reducing wind speed from 10 m s^{-1} (C1) to 5 m s^{-1} (C5). As the wind speed is reduced, each particle falls more vertically and its overall horizontal travel is reduced. Thus, as the wind speed is reduced, each particle is swept over fewer terrain wavelengths and, therefore, each trajectory exhibits less waviness.

As shown in Table 3, the maximum values of the ratios u'/U and w'/U remain constant as the basic wind speed, U, is reduced; however, the values of u' and w' are actually reduced by half. It follows that as wind speed is reduced, particle accelerations are lessened and trajectory focusing is less evident. As shown in Table 3, however, reducing the wind speed changes the wave regime from evanescent (C1) to vertically propagating waves (C5). As shown previously, vertically propagating waves are more effective at producing concentrated particle streams than are evanescent waves. Thus, these two effects tend to cancel, and as a result there is little trajectory convergence in either case.

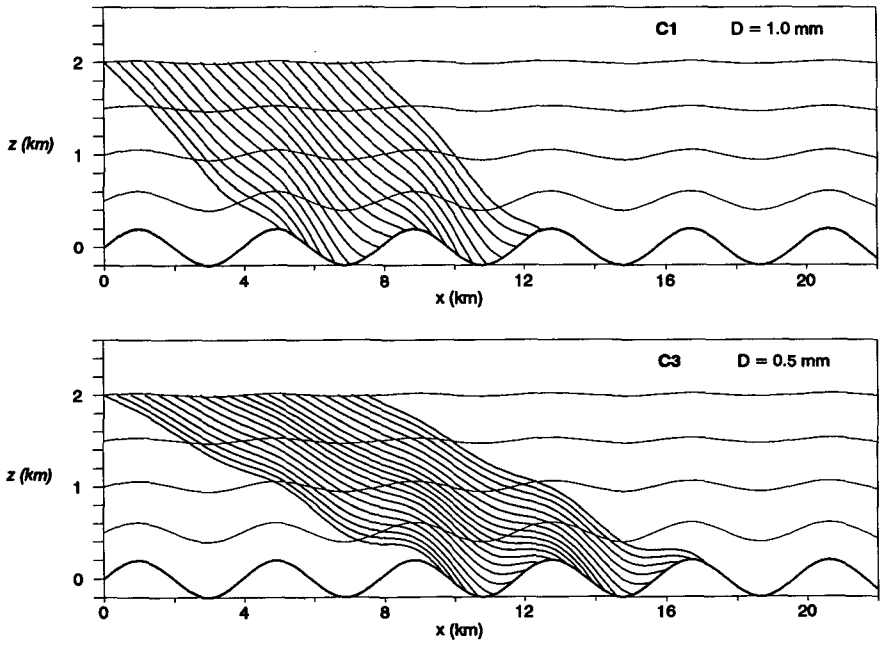

FIG. 6. Effect of particle size on particle trajectories for evanescent waves.

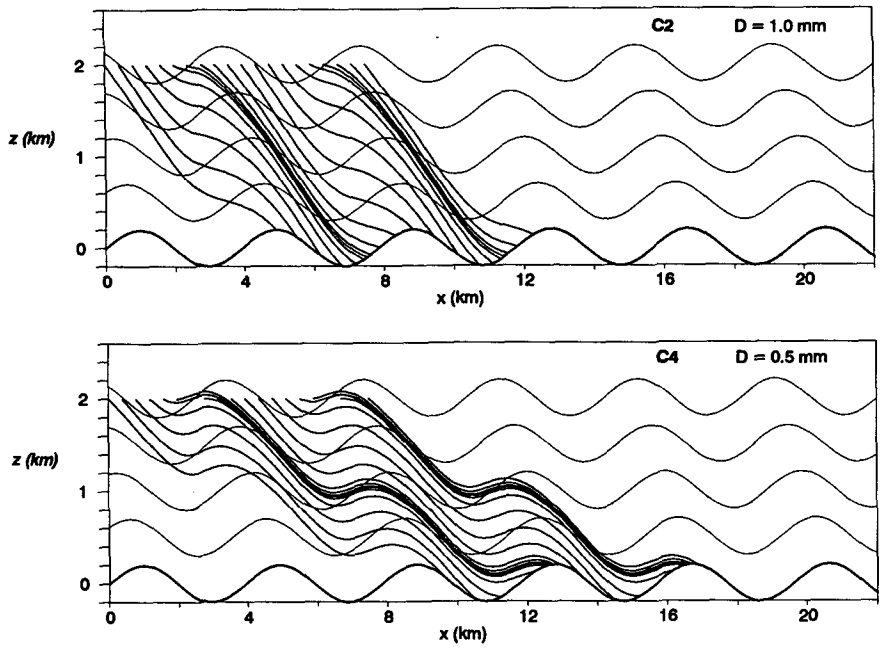

FIG. 7. Effect of particle size on trajectories for vertically propagating waves.

d. Effect of terrain wavelength

In Fig. 9, cases C1 and C6 differ only in the length of the terrain wavelength, L. Doubling the terrain wavelength from 4 to 8 km while maintaining the same hill height has two important effects. First, it reduces the maximum slope of each hill, which considerably reduces the maximum values of u'/U and w'/U, as shown in Table 3. Second, it changes the regime of wave propagation from evanescent to vertically propagating waves.

The effect of changing wave regime, as shown previously, is to increase trajectory focusing. At the same time, the effect of reducing u'/U and w'/U is to reduce

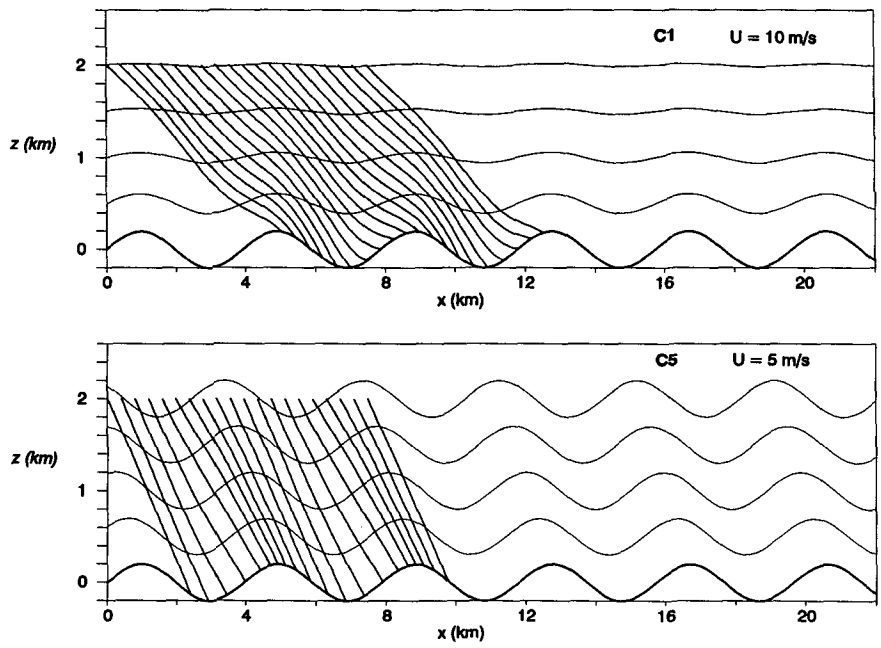

FIG. 8. Effect of wind speed on particle trajectories over sinusoidal terrain.

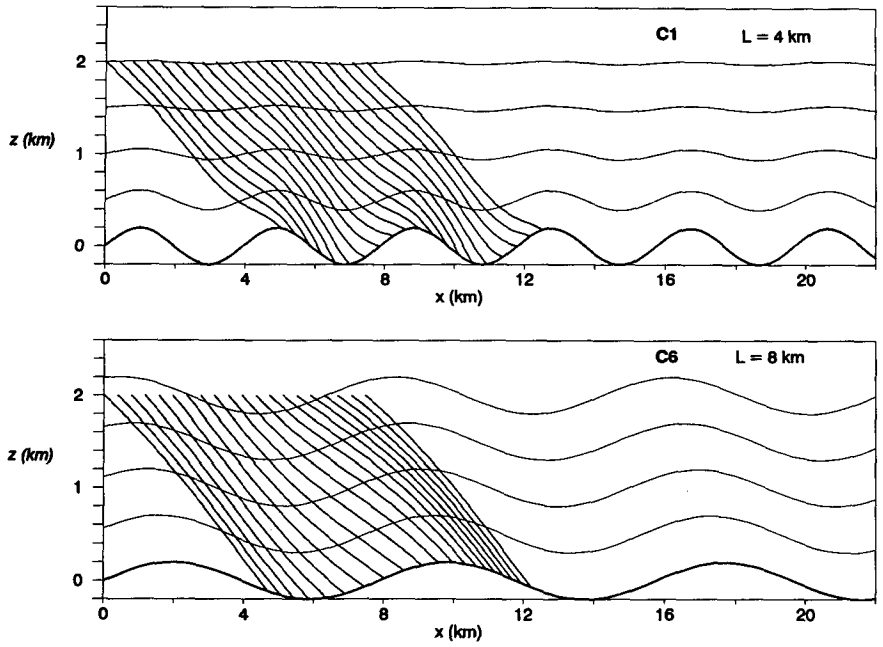

FIG. 9. Effect of terrain wavelength on particle trajectories.

the magnitude of the unsteady aerodynamic forces and, thereby, lessen trajectory focusing. Again, these two effects tend to cancel and the result is only a slight amount of trajectory focusing near the lee side of the hilltop in case C6.

4. Concluding remarks

For the relatively simple case of steady and uniform flow over flat terrain, particles are advected horizontally by the basic wind and descend vertically at their terminal velocity. Thus, each particle tends to fall at a constant speed, along a straight-line trajectory that forms a constant angle with the surface. The angle of fall can be determined simply and analytically.

Particles falling through a spatially varying wind field above complex terrain experience an aerodynamic force of constantly changing magnitude and direction. The unsteady aerodynamic forces deflect particles from otherwise straight-line trajectories.

Numerical simulations of falling particles over sinusoidal terrain have revealed a number of interesting patterns of particle deposition. In some cases, large differences in deposition patterns have resulted from fairly modest changes of a single variable. The following is a summary of the simulation results.

- Stratification significantly affects the flow field, which then controls the pattern of particle deposition. Under strongly stratified conditions, such as that in C2, the presence of vertically propagating waves and the associated upstream phase tilt produces concentrated particle streams. For weakly stratified conditions, such as that in C1, no concentrated particle streams are evident.
- Smaller particles of similar density fall more slowly. As a result, smaller particles spend more time in the air and are carried farther downrange. There is generally more waviness in the trajectories as the particle size is decreased, since each particle travels across additional terrain wavelengths before landing. For evanescent waves, shown in C1 and C3, there is no significant trajectory convergence for either particle size. For vertically propagating waves, shown in C2 and C4, there is significant trajectory focusing for both particle sizes.
- Reducing the wind speed allows particles to fall more vertically, shortening the overall horizontal distance of travel for each particle. There is less waviness in the trajectories as the wind speed is decreased, since each particle travels across fewer wavelengths before setting down on the surface. Reducing the wind speed can change the wave regime from evanescent to vertically propagating waves, yet at the same time perturbation velocities u' and w' are decreased. The former tends to increase trajectory convergence while the latter tends to decrease trajectory convergence.
- Increasing the wavelength of the terrain while maintaining the same amplitude can change the wave regime from evanescent to vertically propagating waves and at the same time considerably reduce u'/U and w'/U. The effect of changing wave regime in this way is to increase trajectory focusing, yet reducing pertur-

bation velocities tends to reduce trajectory convergence. Thus, the two effects tend to cancel and the result is only a slight amount of trajectory focusing when the terrain wavelength is doubled.

In this study, we have made several simplifications, such as uniform basic wind, constant Brunt–Väisälä frequency, and small amplitude sinusoidal hills. This allows us to obtain some physical insight into an otherwise complex problem. Many of these restrictions may be removed by developing a more sophisticated theory or numerical model for the flow field. For example, the present method of calculating particle trajectories could be linked to a fully nonlinear numerical simulation of the flow field. This would allow more flexibility when choosing the type of topography and atmospheric conditions.

Another aspect of flow across topography that is ignored by linear models is the boundary layer. Particles must pass through a boundary layer before impacting the surface. While passing through a boundary layer, particles experience a region of strong wind shear and turbulence. The degree of boundary-layer influence on particle motion will depend on many factors, including the particle's physical characteristics, the boundary-layer structure, and the amount of time the particle is within the boundary layer. To investigate this aspect of the problem, it will be necessary to develop a fairly detailed boundary-layer model that will provide random fluid velocity fluctuations, which then may be translated by the particle dynamics model into the proper particle motion.

Acknowledgments. This research has been supported by the U.S. Environmental Protection Agency under the Cooperative Agreement CR 817931 with North Carolina State University. The contents of this paper do not necessarily reflect the views and policies of the Agency, nor does mention of trade names or commercial products constitute endorsement or recommendation for use.

REFERENCES

Cotton, C. A., 1944: *Volcanoes as Landscape Forms.* Whitcombe & Tombs, 416 pp.

Greeley, R., and J. D. Iversen, 1985: *Wind as a Geological Process.* Cambridge University Press, 333 pp.

Gunn, R., and G. D. Kinzer, 1949: The terminal velocity of fall for water droplets in stagnant air. *J. Meteor.,* **6,** 243–249.

Hobbs, P. V., R. C. Easter, and A. B. Fraser, 1973: A theoretical study of the flow of air and fallout of solid precipitation over mountainous terrain: Part II. Microphysics. *J. Atmos. Sci.,* **30,** 813–823.

Morsi, S. A., and A. J. Alexander, 1972: An investigation of particle trajectories in two-phase flow systems. *J. Fluid Mech.,* **55,** part 2, 193–208.

Pasquill, F., 1974: *Atmospheric Diffusion.* 2d ed. Ellis Horwood, 429 pp.

Queney, P., 1947: Theory of perturbations in stratified currents with applications to airflow over mountain barriers. Department of Meteorology, University of Chicago, Misc. Rep. No. 23.

Smith, R. B., 1979: The influence of mountains on the atmosphere. *Advances in Geophysics,* Vol. 21, Academic Press, 87–230.